

Cavitand–Porphyrins

Stephen D. Starnes, Dmitry M. Rudkevich,* and Julius Rebek, Jr.*

*Contribution from The Skaggs Institute for Chemical Biology and The Department of Chemistry, The Scripps Research Institute, MB-26, 10550 North Torrey Pines Road, La Jolla, California 92037**Received January 3, 2001*

Abstract: The synthesis and characterization of new nanoscale container molecules **7** and **8** are described. They are covalent hybrids of deepened, self-folding cavitands and metalloporphyrins. In receptor **7**, the Zn-porphyrin wall is directly built onto the cavitand skeleton. Host **8** features a large unimolecular cavity containing two cavitands attached with the Zn-porphyrin wall. Its dimensions, $\sim 10 \times 25 \text{ \AA}$, place it among the largest synthetic hosts prepared to date. A series of adamantyl- and pyridyl-containing guests **14–20** of various lengths were prepared and used to determine the hosts' binding abilities in solution using UV/vis and ^1H NMR spectroscopy. Intramolecular hydrogen bonds at the upper rims of the cavitands resist the unfolding of the inner cavities and thereby increase the energetic barrier to guest exchange. The exchange is slow on the NMR time scale (at $\leq 300 \text{ K}$), and kinetically stable complexes result. When the cavities and metalloporphyrins participate simultaneously in the binding event, very high affinities for guests are found ($-\Delta G^{295}$ up to 10 kcal mol^{-1} in toluene), to which the porphyrin fragments contribute significantly ($-\Delta G^{295}$ up to 6 kcal mol^{-1}). The pairwise selection of two different guests by molecular container **8** is reported, and the termolecular complex formed raises the possibility of metal-catalyzed bimolecular reactions in these containers.

Introduction

Synthetic molecular cavities are designed to more or less completely surround smaller molecular guests. The motivations for engineering the cavities depend on the tastes and appetites of the researcher but frequently include molecular recognition, sensing, delivery, and catalysis.^{1–3} However, compared to alternatives such as imprinted polymers,⁴ catalytic antibodies,⁵ liposomes,⁶ and zeolites⁷ the accomplishments are modest, even by the accommodating standards of the community. The moderate dimensions of the synthetic cavities represent the most serious limitations. First carcerands—the container-molecules with enforced interiors^{1a,b}—accommodated only one benzene-sized guest. The more guest-accessible, self-assembling capsules—“tennis balls”,⁸ calix[4]arene tetraureas,⁹ etc. — also generally

encapsulated a single guest molecule, while catalysis most often requires two molecules placed in close proximity. A second, related limitation is functionality: how to provide space for a guest or two *and* a functional group positioned to influence their behavior? Here the central theme is the functionalization of concave surfaces.

There has been progress on the problem of size. Very large hemicarcerands **1** and **2** (Figure 1) were synthesized by Cram¹⁰ and Reinhoudt,¹¹ respectively, in the mid 1990s, and at $\sim 20 \text{ \AA}$ long, they are even now among the largest of unimolecular cavities. Fullerene C_{60} and tetraphenylporphyrin appear ideal guests for **1**, while tetraphenylporphyrin, phthalocyanine, medium-sized dibenzocrown ethers, and steroids can fit nicely within the interior of **2**. But attempts to sequester these large guests in solution failed.^{10,11} Sherman et al. prepared “giant carceplex” **3** that incarcerated three DMF guest-molecules (Figure 1).¹² Subsequently, the same researchers developed an approach toward bis-capsules **4** (Figure 1) which entrapped two different guests—EtOAc, benzene, THF, pyrazine, 1,4-dioxane, etc.—one per each cavity.¹³ The ^1H NMR chemical shifts of the encapsulated species were clearly dependent on the presence of the other guest in the neighboring cavity. Subsequently, nanoscale self-assembled capsules have been synthesized which reversibly bind a single sizable guest or even several guests.¹⁴

There is much less progress on interior functionality. Mo-

(1) (a) Cram, D. J.; Cram, J. M. *Container Molecules and their Guests*; Royal Society of Chemistry: Cambridge, 1994. Carcerands and hemicarcerands: (b) Jasat, A.; Sherman, J. C. *Chem. Rev.* **1999**, *99*, 931–967. (c) Warmuth, R.; Yoon, J. *Acc. Chem. Res.* **2001**, *34*, 95–105. Cryptophanes: (d) Collet, A.; Dutasta, J.-P.; Lozach, B.; Canceill, J. *Top. Curr. Chem.* **1993**, *165*, 103–129. Cyclophanes: (e) Diederich, F. *Cyclophanes*; Royal Society of Chemistry: Cambridge, 1991. Calixarene-based devices: (f) Ikeda, A.; Shinkai, S. *Chem. Rev.* **1997**, *97*, 1713–1734. Catalysts: (g) Sanders, J. K. M. *Chem.—Eur. J.* **1998**, *4*, 1378–1383.

(2) Self-assembled capsules: (a) Conn, M. M.; Rebek, J., Jr. *Chem. Rev.* **1997**, *97*, 1647–1668. (b) de Mendoza, J. *Chem.—Eur. J.* **1998**, *4*, 1373–1377.

(3) (a) Rudkevich, D. M.; Rebek, J., Jr. *Eur. J. Org. Chem.* **1999**, 1991–2005. (b) Higler, I.; Timmerman, P.; Verboom, W.; Reinhoudt, D. N. *Eur. J. Org. Chem.* **1998**, 2689, 9–2702. (c) Seel, C.; Vögtle, F. *Angew. Chem., Int. Ed. Engl.* **1992**, *31*, 528–549.

(4) (a) Wulff, G. *Angew. Chem., Int. Ed. Engl.* **1995**, *34*, 1812–1832. (b) Whitcombe, M. J.; Alexander, C.; Vulfson, E. N. *Synlett* **2000**, 911–923. (c) Sellergren, B. *Angew. Chem., Int. Ed.* **2000**, *39*, 1031–1037.

(5) (a) Lerner, R. A.; Bencovic, S. J.; Schultz, P. G. *Science* **1991**, *252*, 659–667. (b) Schultz, P. G.; Lerner, R. A. *Science* **1995**, *269*, 1835–1842. (c) Schultz, P. G. *Proc. Natl. Acad. Sci. U.S.A.* **1998**, *95*, 14590–14591 and references therein.

(6) Lasic, D. D.; Papahadjopoulos, D. *Science* **1995**, *267*, 1275–1276 and literature therein.

(7) Corma, A.; Garcia, H. *J. Chem. Soc., Dalton Trans.* **2000**, 1381–1394.

(8) Branda, N.; Wyler, R.; Rebek, J., Jr. *Science* **1994**, *263*, 1267–1268. (9) Hamann, B. C.; Shimizu, K. D.; Rebek, J., Jr. *Angew. Chem., Int. Ed. Engl.* **1996**, *35*, 1326–1329.

(10) von dem Bussche-Hünnefeld, C.; Bühring, D.; Knobler, C. B.; Cram, D. J. *J. Chem. Soc., Chem. Commun.* **1995**, 1085–1087.

(11) Timmerman, P.; Nierop, K. G. A.; Brinks, E. A.; Verboom, W.; van Veggel, F. C. J. M.; van Hoorn, W.-P.; Reinhoudt, D. N. *Chem.—Eur. J.* **1995**, *1*, 132–143.

(12) Chopra, N.; Sherman, J. C. *Angew. Chem., Int. Ed.* **1999**, *38*, 1955–1957.

(13) Chopra, N.; Naumann, C.; Sherman, J. C. *Angew. Chem., Int. Ed.* **2000**, *39*, 194–196. Also see: Yoon, J.; Cram, D. J. *Chem. Commun.* **1997**, 2065–2066.

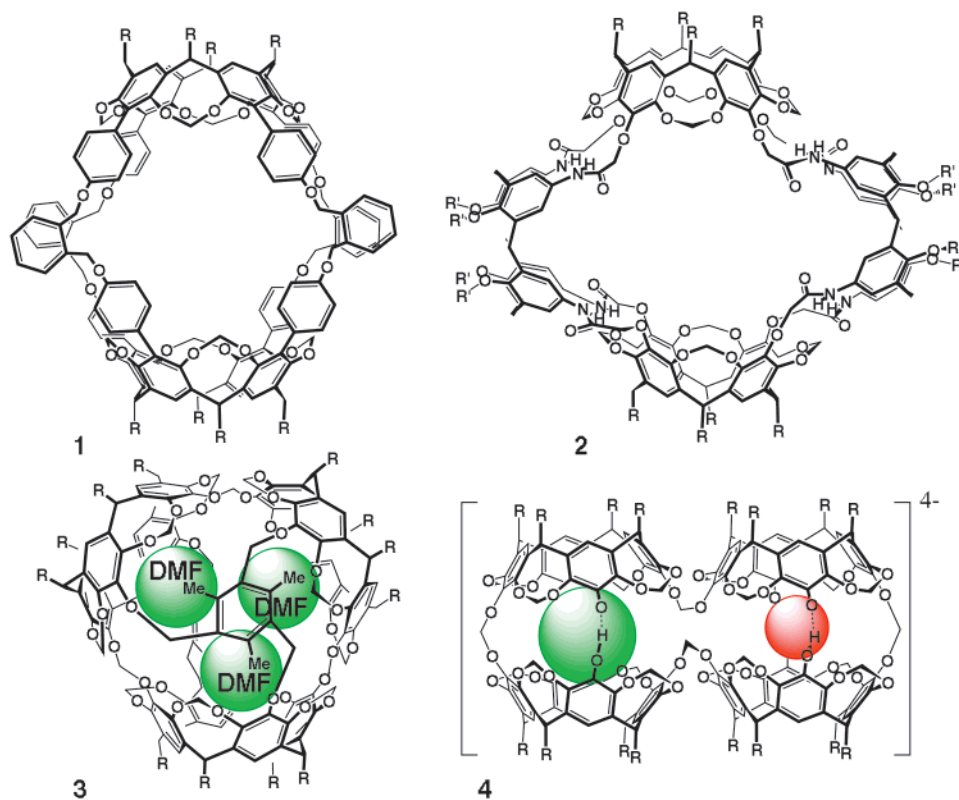


Figure 1. Nanoscale unimolecular cavities 1–4 of a first generation.

molecular clefts, concave reagents, and endohedral functions all testify to the existence of the problem¹⁵ but fail to provide independent binding and functional group sites. An “introverted” carboxyl group derived from Kemp’s triacid and a cavitant¹⁶ appears to provide such an environment and shows a special behavior in the complexation of amines. Here we examine other functions—metalloporphyrins. Although porphyrins have been attached to almost every type of macrocycle in seemingly every type of way,^{17,18} their positioning on the host structures developed below is uniquely suited for assessing the independent contributions of the cavitant and porphyrin to the recognition of guests. We describe here, then, our experiences with hybrids of porphyrins fused to the self-folding cavitants.

The parent cavitant is so-called self-folding cavitant **5** (Figure 2), in which the cyclic array of eight intramolecular secondary amide $C=O \cdots H-N$ hydrogen bonds holds the four aromatic walls together and stabilizes the “vase-like” conformation shown.¹⁹ The circle of hydrogen bonds resists the unfolding of the vase required for guest exchange. This results in a slow

exchange between complexed and free guest species in solution on the NMR time scale. Resonances for the complexed guest species such as adamantanes, lactams, and cyclohexanes are observed upfield of 0 ppm, as expected for inclusion in a shielded magnetic environment, and their orientation in the cavity and the stoichiometry of the complexes are easily deduced. When two self-folding cavitants are covalently attached, a rigid cylindrical host **6** (Figure 2) results, of nanoscale dimensions: $10 \times 23 \text{ \AA}$ and $\sim 800 \text{ \AA}^3$ internal volume.²⁰ The molecule resembles hemicarcerands, but the internal cavity is held by a seam of intramolecular $C=O \cdots H-N$

(14) (a) MacGillivray, L. R.; Atwood, J. L. *Nature* **1997**, *389*, 469–472. (b) Körner, S. K.; Tucci, F. C.; Rudkevich, D. M.; Heinz, T.; Rebek, Jr.; *J. Chem.-Eur. J.* **2000**, *6*, 187–195. (c) Lützen, A.; Renslo, A. R.; Schalley, C. A.; O’Leary, B. M.; Rebek, Jr., Jr. *J. Am. Chem. Soc.* **1999**, *121*, 7455–7456. (d) Cho, Y. L.; Rudkevich, D. M.; Rebek, Jr., Jr. *J. Am. Chem. Soc.* **2000**, *122*, 9868–9869. (e) Fox, O. D.; Drew, M. G. B.; Wilkinson, E. J. S.; Beer, P. D. *Chem. Commun.* **2000**, 391–392. (f) Gerkensmeier, T.; Iwanek, W.; Agena, C.; Fröhlich, R.; Kotila, S.; Näther, C.; Mattay, J. *Eur. J. Org. Chem.* **1999**, 2257, 7–2262. For other covalently linked nanosize host-molecules, see: (g) Higler, I.; Timmerman, P.; Verboom, W.; Reinhoudt, D. N. *J. Org. Chem.* **1996**, *61*, 5920–5931. (h) Higler, I.; Verboom, W.; van Veggel, F. C. J. M.; de Jong, F.; Reinhoudt, D. N. *Liebigs Ann./Recl.* **1997**, 1577–1586. (i) Gibb, C. L. D.; Stevens, E. D.; Gibb, B. C. *Chem. Commun.* **2000**, 363–364.

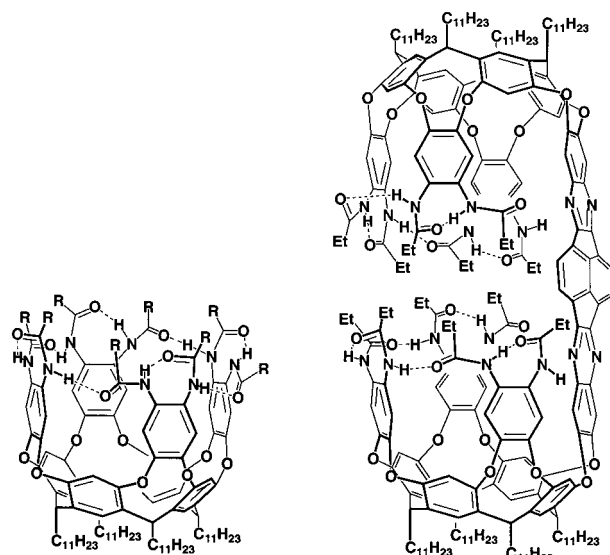
(15) Clefts: Rebek, Jr., *J. Angew. Chem., Int. Ed. Engl.* **1990**, *29*, 245–255. Molecular bowls and capsules with an endohedral functionality: Goto, K.; Okazaki, R. *Liebigs Ann./Recl.* **1997**, 2393–2407. Concave reagents: Lüning, U. *J. Mater. Chem.* **1997**, *7*, 175–182.

(16) Renslo, A. R.; Rebek, Jr., *J. Angew. Chem., Int. Ed.* **2000**, *39*, 3281–3283.

(17) Cyclodextrin-porphyrins: (a) Kuroda, Y.; Hiroshige, T.; Sera, T.; Shiroiwa, Y.; Tanaka, H.; Ogoshi, H. *J. Am. Chem. Soc.* **1989**, *111*, 1912–1913. (b) Kuroda, Y.; Ito, M.; Sera, T.; Ogoshi, H. *J. Am. Chem. Soc.* **1993**, *115*, 7003–7004. Steroid-capped porphyrins: (c) Bonar-Law, R. P.; Sanders, J. K. M. *J. Am. Chem. Soc.* **1995**, *117*, 259–271. (d) Bonar-Law, R. P.; Sanders, J. K. M. *J. Chem. Soc., Perkin Trans. 1* **1995**, 3085–3096. Calixarene-porphyrins: (e) Rudkevich, D. M.; Verboom, W.; Reinhoudt, D. N. *Tetrahedron Lett.* **1994**, *35*, 7131–7134. (f) Rudkevich, D. M.; Verboom, W.; Reinhoudt, D. N. *J. Org. Chem.* **1995**, *60*, 6585–6587. (g) Nagasaki, T.; Fujishima, H.; Takeuchi, M.; Shinkai, S. *J. Chem. Soc., Perkin Trans. 1* **1995**, 1883–1888. Glycoluril-porphyrins: (i) Reek, J. N. H.; Rowan, A. E.; Crossley, M. J.; Nolte, R. J. M. *J. Org. Chem.* **1999**, *64*, 6653–6663. (j) Elemans, J. A. A. W.; Claase, M. B.; Aarts, P. P. M.; Rowan, A. E.; Schenning, A. P. H. J.; Nolte, R. J. M. *J. Org. Chem.* **1999**, *64*, 7009–7016. Cyclophane-porphyrins: (k) Benson, D. R.; Valentekovich, R.; Knobler, C. B.; Diederich, F. *Tetrahedron* **1991**, *47*, 2401–2422. Cyclic arrays of metalloporphyrins: (l) Anderson, S.; Anderson, H. L.; Bashall, A.; McPartlin, M.; Sanders, J. K. M. *Angew. Chem., Int. Ed. Engl.* **1995**, *34*, 1096–1099. Here, high kinetic and thermodynamic stability of the complexes was demonstrated, however, through multiple ligand–metal interactions.

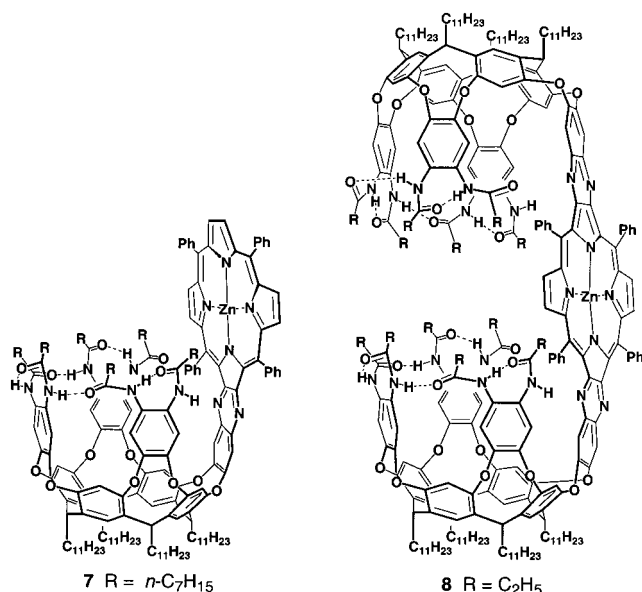
(18) Diels–Alder reactions within cyclic, open-ended metalloporphyrin hosts: (a) Nakash, M.; Clyde-Watson, Z.; Feeder, N.; Davies, J. F.; Teat, S. J.; Sanders, J. K. M. *J. Am. Chem. Soc.* **2000**, *122*, 5286–5293. (b) Nakash, M.; Sanders, J. K. M. *J. Org. Chem.* **2000**, *65*, 7266–7271.

(19) (a) Rudkevich, D. M.; Hilmersson, G.; Rebek, Jr., Jr. *J. Am. Chem. Soc.* **1998**, *120*, 12216–12225. (b) Rudkevich, D. M.; Hilmersson, G.; Rebek, Jr., Jr. *J. Am. Chem. Soc.* **1997**, *119*, 9911–9912. (c) Ma, S.; Rudkevich, D. M.; Rebek, Jr., Jr., *Angew. Chem., Int. Ed.* **1999**, *38*, 2600–2602.



5 R = *n*-C₇H₁₅, CH₂Cl, *cyclo*-C₆H₁₁ 6

Figure 2. Self-folding container-molecules 5 and 6.



7 R = *n*-C₇H₁₅

8 R = C₂H₅

Figure 3. Cavitand–porphyrins 7 and 8.

hydrogen bonds rather than covalent bonds. Access to the cavity is facile under ambient conditions, and the uptake and release of guests is reversible. High kinetic stability of the complexes was achieved for long (~ 18 Å) and rigid adamantyl- and cyclohexyl-containing guests. The new cavitand–porphyrin hybrids are 7 and 8 possessing one or even two deepened self-folding cavities and a metalloporphyrin wall (Figure 3). The Zn-porphyrin fragment presents an additional, strong binding functionality for pyridine bases, so that caviplaxes of unprecedented kinetic and thermodynamic stability result with guests able to interact with both sites.²¹ Moreover, semi-capsule 8 is among the largest of synthetic unimolecular hosts, featuring cavity dimensions of 25×10 Å.

(20) (a) Tucci, F. C.; Renslo, A. R.; Rudkevich, D. M.; Rebek, J., Jr. *Angew. Chem., Int. Ed.* **2000**, *39*, 1076–1079. (b) Lücking, U.; Tucci, F. C.; Rudkevich, D. M.; Rebek, J., Jr. *J. Am. Chem. Soc.* **2000**, *122*, 8880–8889.

(21) Preliminary communication: Starnes, S. D.; Rudkevich, D. M.; Rebek, J., Jr. *Org. Lett.* **2000**, *2*, 1995–1998.

Results and Discussion

Synthesis (Scheme 1, Scheme 2). The synthesis of 7 and 8 starts with the versatile diamine cavitands 9a and 9b. These were described earlier in the context of nanoscale structure 6.²⁰ In short, 9a,b were prepared by partial bridging of the hydroxyls in the parent resorcinarene with three 1,2-dinitrophenylene walls, followed by reduction of the NO₂ groups. Acylation of the resulting amino groups with either *n*-octanoyl or *n*-propanoyl chloride gave the respective hexaamides. Now, by adding the fourth, 1,2-dinitrophenylene wall and reduction of the NO₂ groups, much as described for the other three, the final *o*-phenylene diamine is in place. Condensation of 9a with porphyrin dione 10²² in hot anhydrous toluene afforded the metal-free porphyrin in 43% yield. Subsequent metalation with Zn(OAc)₂ in refluxing CHCl₃/MeOH readily gave 7 as the only product. Bis-cavitand 8 was prepared in the same way from diamine 9b and porphyrin tetraone 11 and then subsequent metalation. In this reaction the desired C-shaped isomer 8 was obtained together with the S-shaped 8-S, in a $\sim 1:1$ ratio. Prior to the metalation, the isomers were separated by chromatography. The assignment of the C- and S-shaped diastereomers was performed through ¹H NMR spectroscopy with their host–guest complexes and will be described below. The simpler Zn-porphyrin 13 was prepared analogously for comparison purposes. Although 2,3,12,13-tetraone porphyrin 11 is known, no experimental details have ever been published.²³ We therefore developed our own protocols and synthesized 11 through tetrahydroxylation of commercially available tetraphenyl porphyrin with OsO₄,²⁴ followed by oxidation of the resulting tetrahydroxybacteriochlorin 12a,b with *o*-iodoxybenzoic acid (IBX) in DMSO²⁵ (12% total yield). Guest molecules 14–19 were synthesized from the corresponding adamantyl- and pyridyl-containing amines, alcohols, and carboxylic acids using standard coupling protocols (see Experimental Section).

Spectroscopic Properties and Conformational Analysis. According to the extensive FTIR, ¹H and ¹³C NMR spectroscopic studies, molecular modeling, and single-crystal X-ray analysis,^{19,26} the upper rim of self-folding cavitands 5 features a seam of eight intramolecular hydrogen bonds formed by the secondary amide groups. Four longer C=O...H–N hydrogen bonds bridge the neighboring aromatic walls, and four shorter ones fix the orientations of the two amides on a given *o*-phenylenediamine unit. The head-to-tail pattern gives rise to two cycloenantiomers,²⁷ with clockwise and counterclockwise orientation of the amide bonds. The interconversion between these is slow on the NMR time scale in CDCl₃ and aromatic

(22) Beavington, R.; Rees, P. A.; Burn, P. L. *J. Chem. Soc., Perkin Trans. I* **1998**, 2847–2851.

(23) (a) Crossley, M. J.; Govenlock, L. J.; Prashar, J. K. *J. Chem. Soc. Chem. Commun.* **1995**, 2379–2380. (b) Kozyrev, A. N.; Alderfer, J. L.; Dougherty, T. J.; Pandey, R. K. *Angew. Chem., Int. Ed.* **1999**, *38*, 126–128. While this manuscript was already under review, Promarak and Burn published their own synthetic protocol for porphyrin 2,3,12,3-tetraone, see: Promarak, V.; Burn, P. L. *J. Chem. Soc., Perkin Trans. I* **2001**, 14–20.

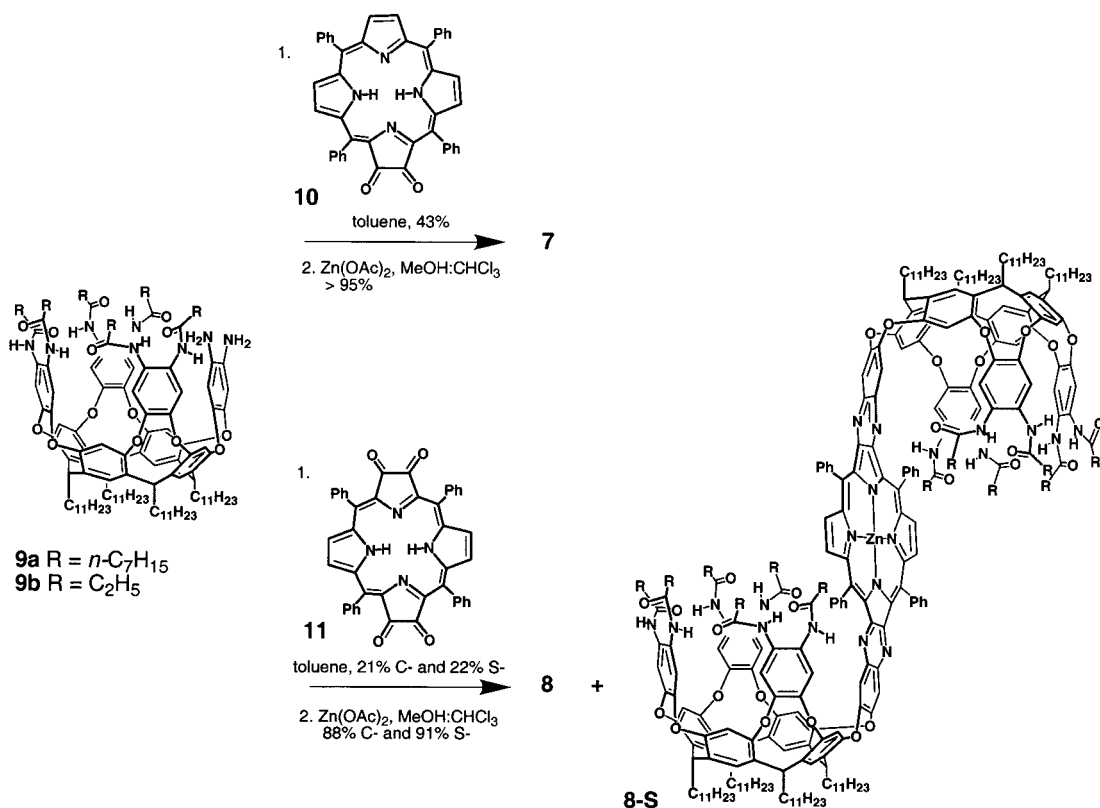
(24) Bruckner, C.; Dolphin, D. *Tetrahedron Lett.* **1995**, *36*, 9425–9428.

(25) Frigerio, M.; Santagostino, M. *Tetrahedron Lett.* **1994**, *35*, 8019–8022.

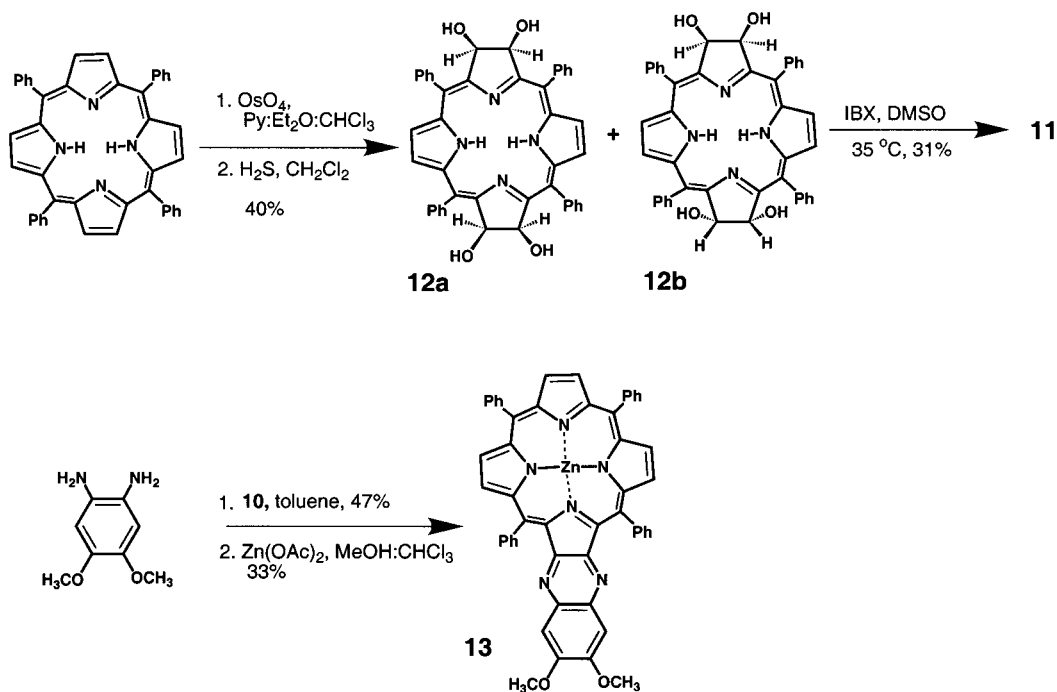
(26) For further structural details (X-ray, ¹H and ¹³C NMR) of self-folding cavitands 5, including the enantiomerically pure compounds, see: Shivanuk, A.; Rissanen, K.; Körner, S. K.; Rudkevich, D. M.; Rebek, J., Jr. *Helv. Chim. Acta* **2000**, *83*, 1778–1790.

(27) Cycloenantiomerism: (a) Prelog, V.; Gerlach, H. *Helv. Chim. Acta* **1964**, *47*, 2288–2294. (b) Goodman, M.; Chorev, M. *Acc. Chem. Res.* **1979**, *12*, 1–7. (c) Yamamoto, C.; Okamoto, Y.; Schmidt, T.; Jäger, R.; Vögtle, V. *J. Am. Chem. Soc.* **1997**, *119*, 10547–10548. In agreement with the Prelog's terminology, enantiomers 5 possess the clock- and counterclockwise "directionality" of the eight secondary amide "building blocks" in an otherwise identical "distribution pattern", or the sequence or connectivity.

Scheme 1



Scheme 2



solvents but fast in more polar solvents. Accordingly, the vase-shaped structure of C_4 symmetry becomes averaged as C_{4v} symmetry in cavitant **5** upon increasing solvent polarity. The ¹H NMR spectrum of cavitant-porphyrin **7** is C_{2v} symmetrical; three methine CH triplets in a 1:2:1 ratio and three porphyrin β-pyrrole singlets in a 1:1:2 ratio are observed (Figure 4b). The C(O)–NH resonances of **7** are found far downfield of 8 ppm (CDCl₃, benzene-*d*₆, and toluene-*d*₈), and the corresponding FTIR spectrum shows hydrogen bonded N–H stretching absorptions at 3240 cm⁻¹ (toluene). Obviously, the secondary

amides form a seam of intramolecular hydrogen bonds, and their arrangements should be cycloenantiomeric: again clockwise or counterclockwise orientation of the head-to-tail amides is possible. The interconversion between the two enantiomers is, however, fast on the NMR time scale (600 MHz, at ≥273 K) since the ¹H NMR spectrum indicates a structure having a plane of symmetry (Figure 4a,b). As in **5**, the characteristic²⁸ methine

(28) (a) Moran, J. R.; Ericson, J. L.; Dalcanale, E.; Bryant, J. A.; Knobler, C. B.; Cram, D. J. *J. Am. Chem. Soc.* **1991**, *113*, 5707–5714. (b) Tucci, F. C.; Rudkevich, D. M.; Rebek, J., Jr. *Chem.–Eur. J.* **2000**, *6*, 1007–1016.

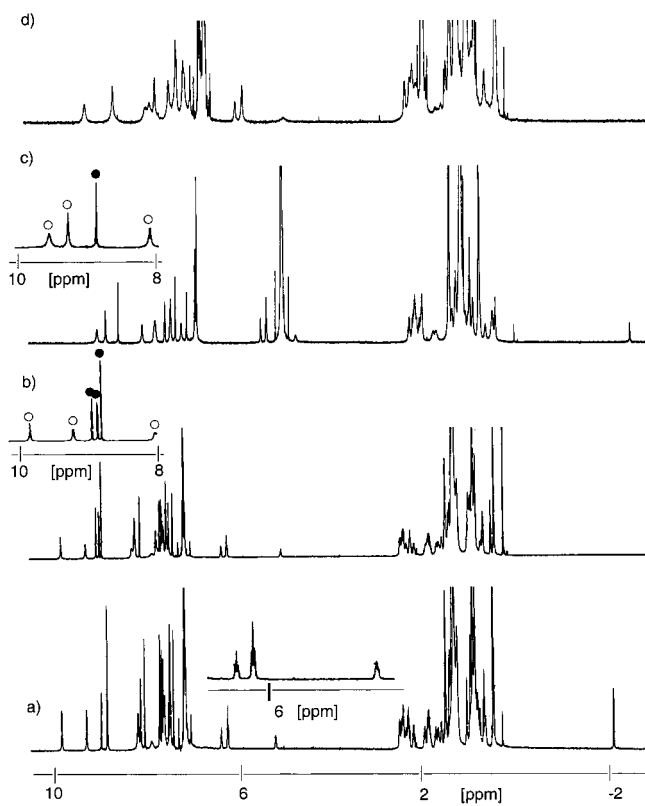


Figure 4. Portions of the ^1H NMR spectra (600 MHz) of: (a) metal-free **7** in benzene- d_6 at 330 K. (b) **7** in benzene- d_6 at 330 K. (c) metal-free **8** in CD_2Cl_2 at 295 K. (d) **8** in toluene- d_8 at 330 K. In the downfield 8–10 ppm region, the amide C(O)NH singlets are marked as “O” and the porphyrin β -pyrrole CH singlets are marked as “●”. The methine CH triplets are situated at 5–6.5 ppm. The porphyrin NH is seen at -2 ppm.

CH signals for the vase-shape are seen at ~ 6 ppm for **7**. The internal cavity dimensions are estimated²⁹ at $9 \times 10 \text{ \AA}$, and the distance between the cavity's bottom and the porphyrin's metal center is $\sim 14 \text{ \AA}$ (Figure 5). From molecular modeling and also by analogy with cavitand **7**, the C(O)–NH amides of each cavity in **8** form a seam of five intramolecular hydrogen bonds within a vase-like structure (Figure 5). Again, the methine CH signals (1:2:1 ratio) are seen at ~ 5.5 –6 ppm, and three C(O)–NH singlets are downfield 8 ppm; only one porphyrin β -pyrrole singlet is observed (Figure 4c,d). Each cycloenantiomeric cavitand in **8** possesses either clockwise or counterclockwise arrangements of the head-to-tail amides. On the other hand, the ^1H NMR spectrum exhibits an average C_{2v} symmetry that indicates the rapid interconversion of the two cycloenantiomers. The internal diameter of **8** was estimated by comparison with **5** and is ~ 9 – 10 \AA ; the internal length of $\sim 25 \text{ \AA}$ was measured from molecular modeling (Figure 5).²⁹

The UV/vis spectra of compounds **7** and **8** are quite different from each other and also from the spectra of normal tetra-arylporphyrins; the conjugated quinoxaline fragment(s) change the symmetry of the porphyrin. Thus, molecule **7** shows a broad Soret band with two maxima at 412 and 450 nm and two Q-bands at 570 and 612 nm, while molecule **8** exhibits large bands at 415 and 470 nm (Soret) and small absorption at 555, 605 (Q-bands), and 657 nm.

Host–Guest Properties. Binding studies with **7** and **8** were performed in toluene solution using UV/vis and ^1H NMR

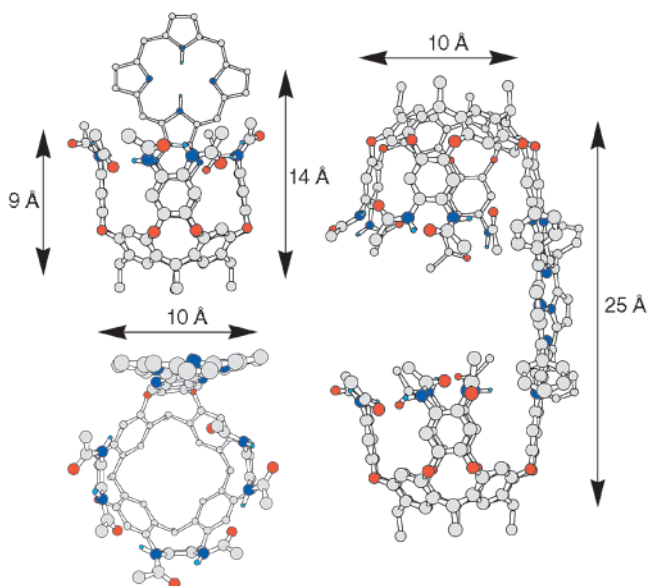


Figure 5. Energy-minimized structures (Amber* Force Field, MacroModel 7.0 program) of host **7** (left, side and top views) and **8** (right, side view). The extended porphyrin wall is not involved in hydrogen bonding. Long alkyl chains and CH bonds have been omitted for viewing clarity. For all cases, only one cycloenantiomeric arrangement is depicted.

spectroscopy. In general, the cavities of **7** and **8** possess typical^{18–20} affinities toward adamantanes, and the Zn-porphyrin wall strongly complexes pyridines.¹⁷ A series of amide/ester-linked guests, **14**–**20** (Figure 6), containing either adamantyl, pyridyl, or both fragments were used in binding assays. Upon complexation, both the UV/vis and the ^1H NMR spectra of hosts **7** and **8** undergo changes (Figures 7 and 8). In the UV/vis spectra, both Soret and Q-bands shift bathochromic. In particular, the Soret band of **7** at 412 nm shifts to ~ 430 nm upon complexation, while the Soret band of **8** at 470 nm shifts to ~ 480 nm. Clear isosbestic points were found in the UV/vis spectra upon titration, and integration of the corresponding NMR spectra indicated a 1:1 stoichiometry for the complexes. Slow exchange between the free and complexed guests **16**–**19** was observed on the NMR time scale already at room temperature. The bound guest signals were seen upfield of 0 ppm at ≤ 300 K. For the complexed 1-substituted adamantanes **16**–**19**, all four signals of the skeleton protons were clearly seen between 0 and -2 ppm. The functional group at the adamantane's 1-position is generally not shifted upfield in the NMR spectra, indicating that the adamantane skeleton is oriented toward the bottom of the cavity in **7** and **8**. The pyridyl signals of the complexed guest were also seen shifted ~ 2 – 3 ppm upfield.

Neither model adamantane **14** nor model pyridine **15** showed kinetically stable binding to **7** at 295 K (UV/vis, NMR control). However, at 273 K, $\ln K_{\text{ass}} = 5.0$ and $-\Delta G^{273} = 2.7 \text{ kcal mol}^{-1}$ were determined for the 1:1 complex **7**•**14** from the ^1H NMR spectra in toluene- d_8 . This is in fair agreement with the binding affinities ($\sim 3 \text{ kcal mol}^{-1}$) obtained for the complex **5** with adamantanes.¹⁸ The interaction between the Zn-porphyrin wall and pyridyl group in toluene was estimated from the titrations with **7** and **15** or with model porphyrin **13** and **17b**, respectively. The affinity does not exceed $-\Delta G^{295} \approx 6.0 \text{ kcal mol}^{-1}$.

At the same time, already 0.4 equiv of bidentate adamantyl–pyridyl guest **17b** was enough to give new signals for the complex **7**•**17b** (Figure 8a,b). Both adamantyl and pyridyl signals of the complexed guest were shifted upfield, and separate sets of signals for the free and bound host were apparent.

(29) MacroModel 7.0; Amber* Force Field. See: Mohamadi, F.; Richards, N. G.; Guida, W. C.; Liskamp, R.; Lipton, M.; Caufield, C.; Chang, G.; Hendrickson, T.; Still, W. C. *J. Comput. Chem.* **1990**, *11*, 440–467.

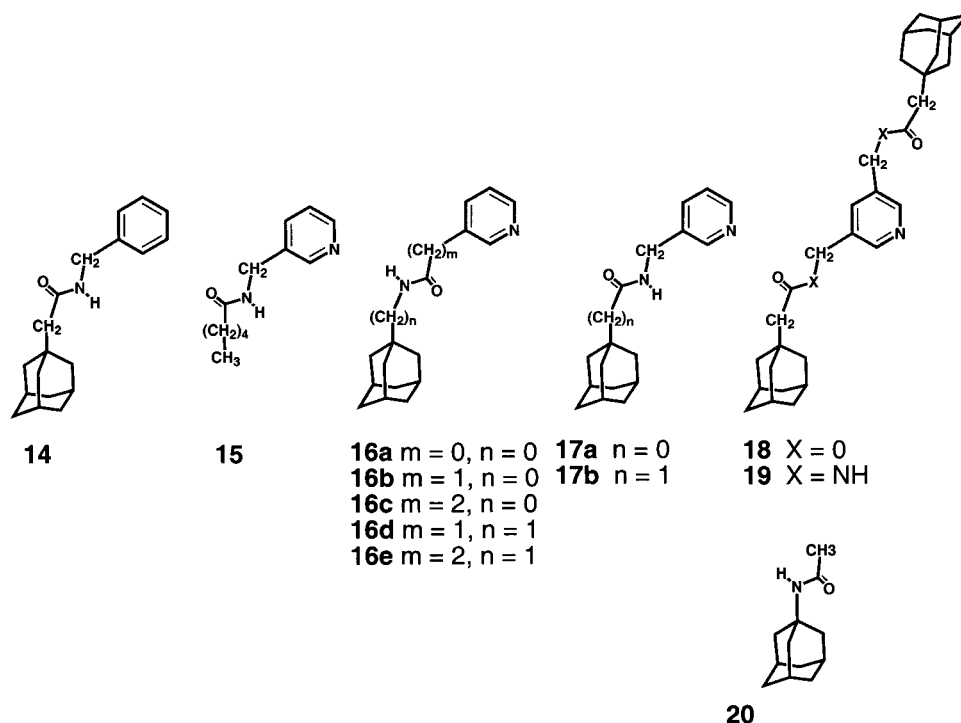
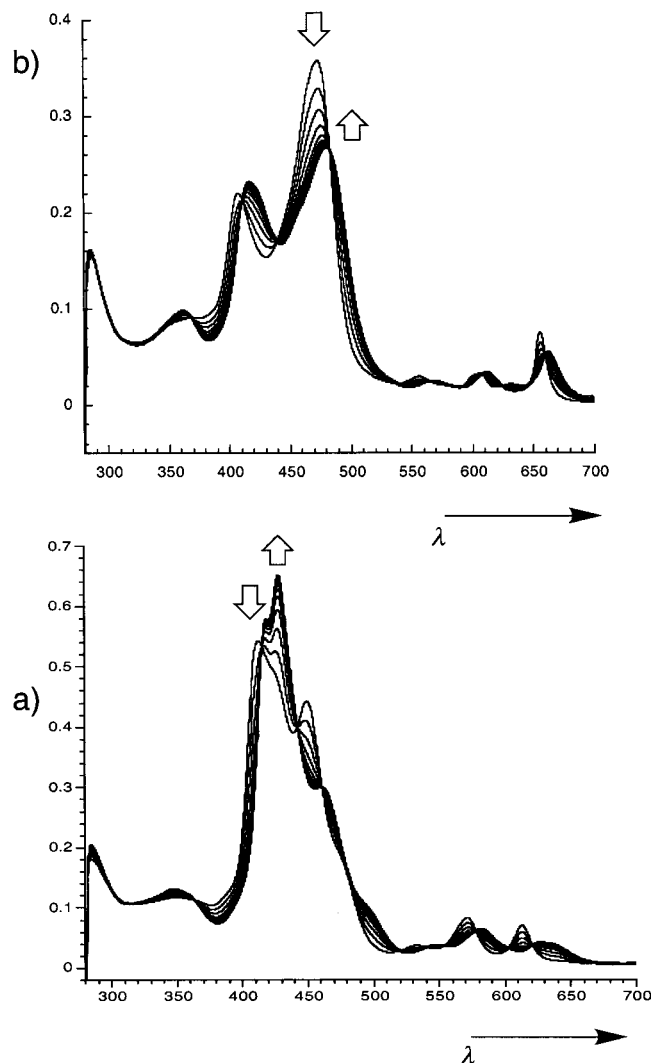
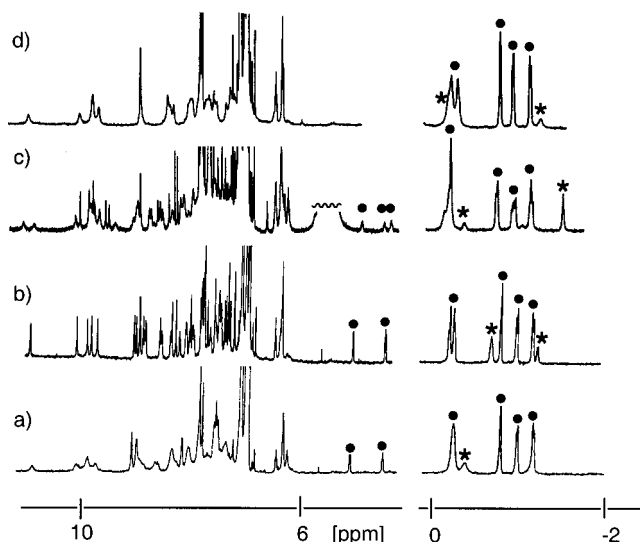


Figure 6. Guest-molecules 14–20.

Figure 7. Portions of the UV/vis titration spectra with guest **17b** (toluene, 295 K): (a) host **7**, (b) host **8**.Figure 8. Downfield and upfield portions of the ^1H NMR spectra (600 MHz, toluene- d_8) of 1:1 complexes: (a) **7**•**17b** at 295 K. (b) **7**•**17b** at 273 K. (c) **8**•**17b** at 273 K. (d) **8**•**19** at 273 K. The complexed guest signals are marked as “●”; the alkyl chain’s CH protons of the cavitand exposed to the porphyrin ring current were assigned through NMR experiments and are marked as “*”.

Accordingly, bidentate 1:1 binding occurred, with the adamantyl fragment held within the cavity of **7** and the pyridine complexed to the metal of the porphyrin wall (Figure 9). The ^1H NMR spectrum of complex **7**•**17b** is rather broad at 295 K, but at ≤ 280 K very sharp signals were observed. All amide N–H signals were seen separately, indicating that the interconversion between the cycloenantiomers within the complex is slow.³⁰

Binding UV/vis studies with **7** and **17b** in toluene gave the association energy of $-\Delta G^{295} = 9.5 \text{ kcal mol}^{-1}$ (Figure 7a and Table 1), reflecting *simultaneous* participation of the cavity and the Zn-porphyrin in the complexation event. Likewise, strong

(30) In guest-free **7**, cycloenantiomers interconvert fast even at lower temperatures.

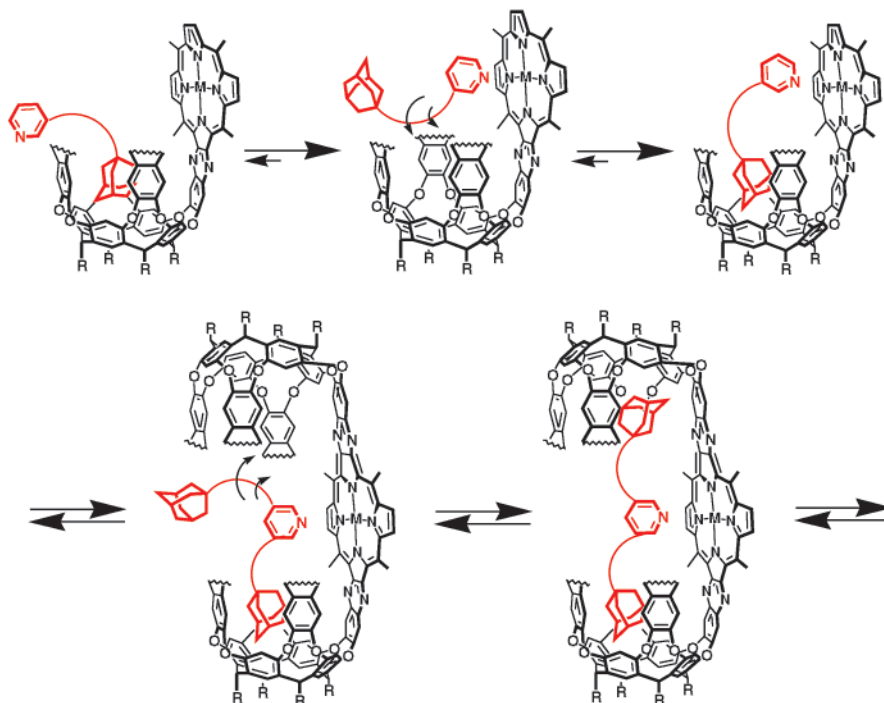


Figure 9. Schematic representation of bidentate binding in cavitand–porphyrins **7** and **8**.

Table 1. Association Constants ($\ln K_{\text{ass}}$) and Binding Energies ($-\Delta G^{295}$, kcal mol $^{-1}$) of Guests **14**–**19** by Porphyrins **7**, **8**, and **13**^{a,b}

complex	$\ln K_{\text{ass}}$	$-\Delta G^{295}$	$\Delta\Delta G^{295}$
7 + 14	<i>c</i>	<i>c</i>	
7 + 15	10.3	6.0	0.0
7 + 16a	10.5	6.1	0.1
7 + 16b	11.8	6.9	0.9
7 + 16c	13.6	7.9	1.9
7 + 16d	12.9	7.5	1.5
7 + 16e	12.0	7.0	1.0
7 + 17a	9.5	5.6	−0.4
7 + 17b	16.2	9.5	3.5
8 + 17b	16.5	9.7	3.7
8 + 18	13.6	7.5	
8 + 19	15.8	9.2	
13 + 17b	8.9	5.2	

^a Determined by UV/vis in toluene at 295 K. [**7**] = [**8**] = [**13**] = 4.5×10^{-6} M, guest concentration 2.0×10^{-6} – 8.0×10^{-5} M. Error $\pm 10\%$. ^b Data collected from at least two independent experiments. ^c No visible complexation was detected by UV/vis in toluene at 295 K. No kinetically stable complex was detected at 295 K by ^1H NMR in toluene-*d*₈. At 273 K, $\ln K_{\text{ass}} = 5.0$ and $-\Delta G^{295} = 2.7$ kcal mol $^{-1}$ was calculated from the ^1H NMR experiment in toluene-*d*₈.

binding ($-\Delta G^{295} = 7.9$ and 7.5 kcal mol $^{-1}$) was detected for adamantyl–pyridines **16c** and **d**, respectively, in which the bound fragments are separated by two methylenes and a secondary amide. This appears to be the optimal length for the spacer; with the shorter **16a,b** and **17a** and longer **16e**, lower binding was measured ($-\Delta G^{295}$ between 5.6 and 7.0 kcal mol $^{-1}$). Here, the cavity contributed less than 1 kcal mol $^{-1}$ to the overall complexation.

Container molecule **8** features cavities that are well preorganized for cooperative binding, and it readily forms kinetically stable complexes with long guests **18** and **19** containing two adamantyl ends with a pyridyl in the center. All four 1-adamantyl signals were clearly observed upfield of 0 ppm (Figure 8c,d), and aided the structure assignment to the C-shaped **8** and the S-shaped diastereomer **8-S**. Specifically, two adamantyl fragments were integrated in the ^1H NMR spectrum of the

complex **8**•**19** and only one adamantyl was seen for the complex **8-S**•**19** ([**8**] = [**8-S**] = [**19**] = 0.5 mM, 270–295 K temperature range).

Binding studies between **8** and monoadamantyl **17b** and bis-adamantyl **18** and **19** guests in toluene showed very strong association: $-\Delta G^{295}$ of 9.7, 7.5, and 9.2 kcal mol $^{-1}$, respectively. (Table). Obviously, the cavities and the Zn-porphyrin wall were involved in the complexation (Figure 9). The fact that diester **18** is less strongly complexed than diamide **19** once again reflects the involvement of the guest's C(O)–NH proton in the hydrogen bonding with the cavity's amide walls.¹⁹ At the same time, the small difference in binding of **17b** versus **19** indicates that the contribution of the second adamantyl is not significant. This may involve the entropic cost of accommodating the more bulky **19** within the inner cavity of **8**.³¹

For the complexed adamantyl–pyridine **17b**, the set of the adamantyl's CH protons was *doubled* (Figures 8c, 10, and 11), along with those of the amide NH's and the aromatics of the host's skeleton. Integration showed only one cavity in **8** was occupied with the adamantane. Accordingly, there are two *diastereomeric* 1:1 complexes **8**•**17b**.

This was not unexpected. As in the topologically similar nanostructures **6**,²⁰ molecule **8** possesses two cycloenantiomeric cavities. In the absence of guests, the interconversion between the two cycloenantiomeric forms is fast (see Figure 4c,d), and the cyclodiastereomers were not thus observed. Upon complexation, the interconversion of **8**•**17b** (and **7**•**17b**!) becomes slow.

Pairwise Guest Selection. In the complex **8**•**17b**, not only the occupied but also the “empty” (e.g., solvated with toluene)

(31) Strong binding was also detected for the S-shaped diastereomer **8-S** and adamantyl–pyridines **17b**, **18**, and **19** (UV/vis, ^1H NMR); the binding energy values ($-\Delta G^{295}$) of 9.9, 6.9, and 9.6 kcal mol $^{-1}$, respectively, were determined. However, unlike C-shaped **8**, addition of more than 1 equiv of these guests to the toluene solution of **8-S** results in a disappearance (!) of kinetically stable complexes in the corresponding ^1H NMR spectra and also causes an additional shoulder in the UV/vis spectra. The guest complexation in **8-S** may equally take place from both sides of the porphyrin plane; such competition apparently results in the faster guest exchange. Similar phenomena have been previously reported by Sanders and co-workers: Hunter, C. A.; Meah, M. N.; Sanders, J. K. M. *J. Am. Chem. Soc.* **1990**, *112*, 5773–5780.

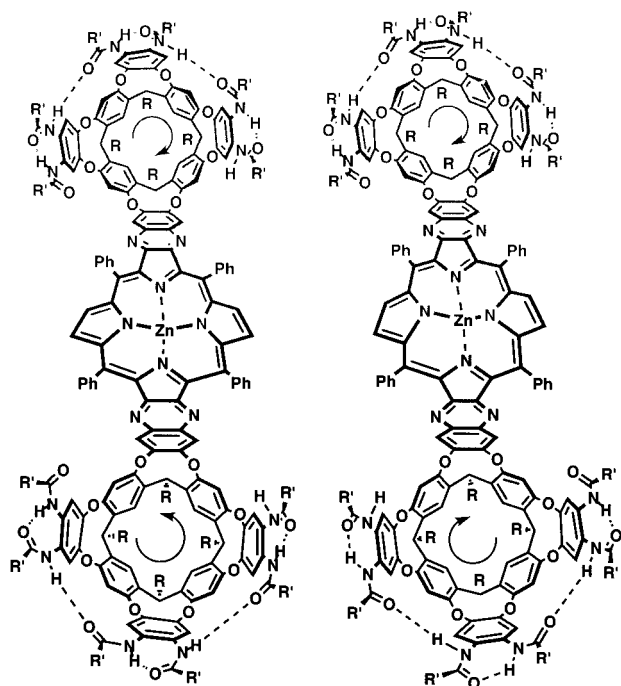


Figure 10. Cartoon representation of cyclodiastereomerism in **8**.

cavity exists as a mixture of cycloenantiomers, and they are in slow NMR exchange. This implies some sort of communication between these cavities. In the ^1H NMR experiment, stepwise addition of *N*-(1-adamantyl)acetamide **20** to the toluene- d_8 solution of complex **8**•**17b** resulted in the disappearance of the doubled set of the adamantyl diastereomeric signals (Figure 11). When ≥ 1 equiv of **20** is added, only one set for all groups of the adamantane CH protons is clearly present. Obviously, guest **20** replaces the toluene molecule from the “empty” cavity of **8**•**17b**; the signals for the encapsulated **20** were observed simultaneously with the encapsulated **17b** upon lowering the temperature to ~ 250 K. It is also known that *N*-(1-adamantyl)-carboxamides accelerate the interconversion of the cycloenantiomeric hydrogen-bonded seams in self-folding cavitands.¹⁹ Accordingly, upon complexation of **20** two cyclodiastereomers are in a fast exchange on the NMR time scale.

More intriguing is the *pairwise selection* of two different guests by molecular container **8** (Figure 12). Complexation of adamantyl-pyridine **17b** produces ~ 9 kcal mol $^{-1}$ of binding energy and doubtlessly replaces one solvent (toluene) molecule

from the interior. The following entrapment of adamantane **20** brings another 2–3 kcal mol $^{-1}$ of energy and releases the second solvent molecule from the remaining cavity. As a result, the ternary complex **17b**•**8**•**20** is formed *quantitatively*.³² In another experiment, both cavities of **8** were first saturated with adamantane **20** (^1H NMR control at 250 K), and then one of the guest molecules was replaced upon addition of 1 equiv of **17b**. As in the previous case, the ternary complex **17b**•**8**•**20** was formed exclusively.

Conclusions and Outlook

Molecular hosts surrounding their guests range from the covalently sealed carcerands to reversibly self-assembled hydrogen-bonded capsules. The unimolecular, deepened cavities in self-folding structures **5**–**8** are in-between in their properties. They are open and bind guests reversibly, but strong and slow on the NMR time scale. The cavities, lined with aromatic surfaces, act as supramolecular NMR shift reagents. The internal space is nanoscale, and the constant flow of substrates into and products out of the cavity may be envisioned in their use as reaction chambers. In the cases at hand, the porphyrin functions contribute to high binding affinities of appropriate guests and raise the possibility of metal-catalyzed reactions—alkane hydroxylations or alkene epoxidations—in these containers. The spectroscopic properties of the porphyrin wall promises energy transfer to the appropriate guest molecules. The stoichiometric pairwise selection of guests is unprecedented for unimolecular hosts, and bimolecular reactions within the shielded interior are likely. The synthesis of water-soluble and polymer-immobilized versions of hosts **7** and **8** is also possible.³³

These applications are currently under exploration and will be reported in due course.

Experimental Section

General. Melting points were determined on a Thomas-Hoover capillary melting point apparatus and are uncorrected. ^1H NMR and ^{13}C NMR spectra were recorded on Bruker DRX-600 spectrometer. Chemical shifts were measured relative to residual nondeuterated solvent resonances. FTIR spectra were recorded on a Perkin-Elmer Paragon 1000 PC FT-IR spectrometer. UV/vis spectra were recorded on a Perkin-Elmer UV/vis Lambda 12 spectrometer. High-resolution matrix-assisted laser desorption/ionization mass spectrometry (HR MALDI FTMS) experiments were performed on a IonSpec HiResMALDI Fourier transform mass spectrometer. For high-resolution mass spectral data of compounds with molecular weight ≥ 2000 , lower than 10 ppm

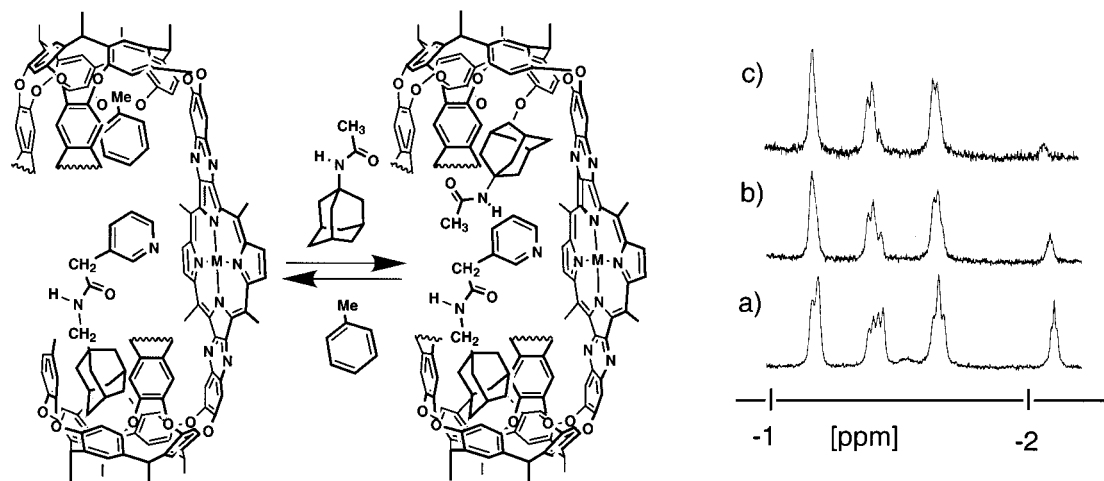


Figure 11. Ternary complex **17b**•**8**•**20**. Upfield portions of the ^1H NMR spectra of the complexes (600 MHz, toluene- d_8 , 273 K): (a) **8**•**17b**. (b) **8**•**17b** and 1 equiv of **20**. (c) **8**•**17b** and 10 equiv of **20**.

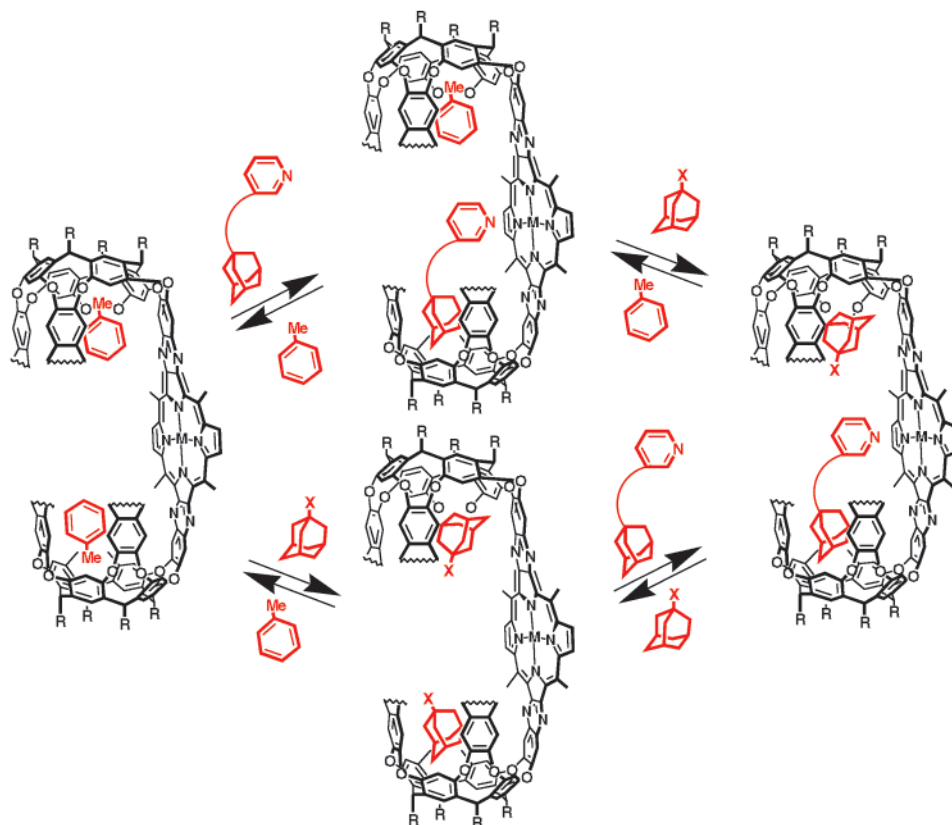


Figure 12. Pairwise selection experiments: a cartoon representation. Two performed routes toward ternary complex **17b•8•20** are shown (^1H NMR experiment, 600 MHz, toluene- d_8 , 250–273 K).

resolution was achieved.³⁴ Column chromatography was performed with Silica Gel 60 (EM Science or Bodman, 230–400 mesh). All experiments with moisture- or air-sensitive compounds were performed in anhydrous solvents under a nitrogen atmosphere. Molecular modeling was performed using the Amber* force field in MacroModel 7.0.²⁹

cis- and trans-2,3,12,13-Tetrahydroxybacteriochlorin, Mixture of Isomers (12a, 12b). OsO_4 (0.5 g, 2.0 mmol) (*toxic!*) was dissolved in diethyl ether (5 mL) and pyridine (2 mL), and the resulting bright-orange solution was added to tetraphenylporphyrin (580 mg, 0.94 mmol) dissolved in CHCl_3 (200 mL). The mixture was stirred in the dark under a nitrogen atmosphere at 25–30 °C for 7 days. The solvent was removed in vacuo, and the solid residue was dissolved in CH_2Cl_2 (250 mL). H_2S was then bubbled through the solution for 15 min. The solution was filtered through Celite; the flask and the Celite layer were rinsed with CH_2Cl_2 (50 mL) and $\text{MeOH}:\text{CH}_2\text{Cl}_2$, 1:9 (200 mL). The solvent was removed in vacuo and the product purified first by extracting the solid residue with CH_2Cl_2 (2 \times 20 mL). The *cis*- and *trans*-tetrahydroxybacteriochlorins **12a,b** are sparingly soluble in CH_2Cl_2 ; thus, the initial extraction provides a rough purification. The product was further purified by column chromatography (gradient ranging from CH_2Cl_2 then 99:1, 98:2, 97:3, and finally 96:4 CH_2Cl_2 :MeOH). The

cis- and *trans*-isomers were separated with R_f (*trans*-) = 0.46 and R_f (*cis*-) = 0.35 (97:3 CH_2Cl_2 :MeOH) as purple solids. Combined yield 257 mg (40%). *cis*-isomer **12a**: ^1H NMR (DMSO- d_6 , 330 K): δ 7.96 (d, 4H, J = 1.8 Hz), 7.92 (br s, 8H), 7.61 (m, 12H), 5.98 (s, 4H), 4.80 (br s, 4 H, OH), -1.52 (s, 2H); ^1H NMR (CDCl_3 , 295 K, 600 MHz): δ 8.13 (s, 4H), 8.07 (d, 4H, J = 6.3 Hz), 7.86 (d, 4H, J = 5.3 Hz), 7.66 (m, 12H), 6.21 (s, 4H), 2.95 (s, 4 H, OH), -1.79 (s, 2H); ^{13}C NMR (CDCl_3 , 295 K, 150 MHz): δ 158.5, 141.2, 137.4, 133.8, 131.9, 128.1, 123.7, 116.0, 74.0; HRMALDI-FTMS m/z 683.2651 ($[\text{M} + \text{H}]^+$, calcd for $\text{C}_{44}\text{H}_{34}\text{N}_4\text{O}_4\text{H}$ 683.2653, error = 0.3 ppm). *trans*-isomer **12b**: ^1H NMR (DMSO- d_6 , 330 K): δ 8.02 (d, 4H, J = 1.6 Hz), 7.89 (br s, 8H), 7.61 (m, 12H), 5.88 (s, 4H), 4.86 (br s, 4 H, OH), -1.63 (s, 2H); ^1H NMR (CDCl_3 , 295 K): δ 8.15 (d, 4H, J = 1.8 Hz), 8.04 (d, 4H, J = 5.0 Hz), 7.85 (br d, 4H), 7.66 (m, 12H), 6.16 (s, 4H), 3.06 (s, 4 H, OH), -1.86 (s, 2H); ^{13}C NMR (CDCl_3 , 295 K, 150 MHz): δ 158.1, 141.2, 137.4, 133.5, 132.1, 128.1, 123.7, 116.1, 74.2; HRMALDI-FTMS m/z 683.2680 ($[\text{M} + \text{H}]^+$, calcd for $\text{C}_{44}\text{H}_{34}\text{N}_4\text{O}_4\text{H}$ 683.2653, error = 4.0 ppm).

Porphyrin 2,3,12,13-Tetraone (11). IBX (492.4 mg, 1.76 mmol) was suspended in DMSO (2 mL) and stirred for 1 h to achieve complete dissolution of the oxidant. A mixture of the *cis*- and *trans*-isomers **12a,b** (150 mg, 0.22 mmol) in DMSO (3 mL) was then added. The reaction mixture was stirred at room temperature, and the course of the conversion was followed by TLC (SiO_2 , 98:2 CH_2Cl_2 :MeOH). After 10–12 h, an additional of IBX (246.2 mg, 0.88 mmol) was added (e.g., 3 equiv of IBX per alcohol), and the mixture was stirred at 50 °C for 2 h and then at room temperature overnight. Water (20 mL) was added, resulting in precipitation of the desired product. The mixture was filtered, and the solid residue was rinsed with water (5 \times 20 mL). The solid residue was then washed with CH_2Cl_2 to extract the porphyrin product. The CH_2Cl_2 solution was evaporated in vacuo, and the product was purified by column chromatography (CH_2Cl_2 , R_f = 0.44) to afford **11** as a purple solid. Yield 46.3 mg (31%, not optimized). Mp > 275 °C; ^1H NMR (CDCl_3 , 295 K): δ 8.49 (s, 4H), 7.81 (d, 8H, J = 7.2 Hz), 7.74 (t, 4H, J = 7.3 Hz), 7.68 (t, 8H, J = 7.3 Hz), -1.86 (s, 2H); ^{13}C NMR (CDCl_3 , 295 K, 150 MHz): δ 186.9, 140.9, 139.6, 138.4,

(32) Size-shape pairwise selection of two different guests by a self-assembled cylindrical capsule: (a) Heinz, T.; Rudkevich, D. M.; Rebek, J., Jr. *Nature* **1998**, *394*, 764–766. (b) Heinz, T.; Rudkevich, D. M.; Rebek, J., Jr. *Angew. Chem., Int. Ed.* **1999**, *38*, 1136–1139. (c) Tucci, F. C.; Rudkevich, D. M.; Rebek, J., Jr. *J. Am. Chem. Soc.* **1999**, *121*, 4928–4929. For the examples from the carcerand chemistry, see ref 13. In steroid-capped porphyrins, see ref 17c.

(33) For the recent synthesis of water-soluble self-folding cavitands, see: Haino, T.; Rudkevich, D. M.; Shivanyuk, A.; Rissanen, K.; Rebek, J., Jr. *Chem.—Eur. J.* **2000**, *6*, 3797–3805. Preliminary results on polymer-supported self-folding cavitands: Rafai Far, A.; Rudkevich, D. M.; Haino, T.; Rebek, J., Jr. *Org. Lett.* **2000**, *2*, 3465–3468.

(34) For details on high-resolution mass spectrometry, see: (a) Rose, M. E.; Johnstone, R. A. W. *Mass Spectrometry for Chemists and Biochemists*; Cambridge University Press: Cambridge, 1982. (b) Jennings, K. R.; Dolnikowski, G. G. *Methods in Enzymology*; McCloskey, J. A., Ed.; Academic Press: New York, 1990; p 37 and references therein.

132.5, 129.0, 128.7, 127.6, 117.4; FTIR (CH₂Cl₂, thin film, cm⁻¹): ν 3426, 3053, 2986, 1728, 1637, 1417; UV/vis [CHCl₃, λ max (log ϵ) 383.9 (5.20), 630.0 (3.58), 774.20 (3.59)]; HRMALDI-FTMS m/z 674.1987 ([M]⁺, calcd for C₄₄H₂₆N₄O₄ 674.1960, error = 4.0 ppm).

Zn-Porphyrin (8). A Typical Procedure. Hexaamide diamine cavitand **9b** (152.7 mg, 0.082 mmol) and tetraone **11** (27.7 mg, 0.041 mmol) were dissolved in anhydrous toluene (20 mL), and nitrogen gas was bubbled through the mixture for 15 min. The mixture was stirred in the dark at 90 °C for 36 h. The solvent was removed in vacuo and the product isolated by column chromatography (eluting with a gradient ranging from CH₂Cl₂ then 99:1, 98:2, and finally 97:3 CH₂Cl₂:MeOH). The S-isomer eluted prior to the C-isomer. The products were then triturated with hexane and MeOH, affording 39 mg of the S-isomer (22%) and 37 mg of the C-isomer (21%) as purple solids. S-isomer: mp > 275 °C; ¹H NMR (CD₂Cl₂, 295 K): δ 9.46 (br s, 4H), 9.28 (br s, 4H), 9.00 (s, 4H), 8.45 (br s, 4H), 8.17 (br s, 8H), 7.95 (t, 4H, J = 7.6 Hz), 7.82 (t, 8H, J = 7.3 Hz), 7.72 (s, 4H), 7.58 (br s, 3H), 7.46 (s, 4H), 7.32–7.22 (m, 22H), 5.80 (t, 2H, J = 8.3 Hz), 5.67 (t, 4H, J = 8.2 Hz), 5.05 (br s, 2H), 2.48–2.14 (m, 32H), 1.9–1.7 (m, 8H), 1.45–0.95 (m, 173H), 0.90–0.80 (m, 34H), 0.80–0.70 (m, 4H), 0.54–0.45 (m, 14H), –2.54 (s, 2H); MALDI-TOF m/z 4318 ([M + H]⁺, calcd for C₂₇₂H₃₂₂N₂₀O₂₈H 4317.4). C-isomer: mp > 275 °C; ¹H NMR (CD₂Cl₂, 295 K): δ 9.47 (br s, 4H), 9.28 (br s, 4H), 8.99 (s, 4H), 8.45 (br s, 4H), 8.17 (br s, 8H), 7.95 (t, 4H, J = 7.7 Hz), 7.82 (br t, 8H), 7.71 (s, 4H), 7.58 (br s, 3H), 7.46 (s, 4H), 7.27–7.24 (m, 22H), 5.79 (t, 2H, J = 8.3 Hz), 5.67 (t, 4H, J = 8.1 Hz), 5.01 (br s, 2H), 2.45–2.13 (m, 32H), 1.9–1.7 (m, 8H), 1.46–0.92 (m, 174H), 0.91–0.80 (m, 34H), 0.80–0.65 (m, 4H), 0.59–0.45 (m, 14H), –2.54 (s, 2H); MALDI-TOF m/z 4318 ([M + H]⁺, calcd for C₂₇₂H₃₂₂N₂₀O₂₈H 4317.4).

The free base S-isomer (20.5 mg, 0.0047 mmol) was added to a solution of Zn(OAc)₂ (7 mg) in CHCl₃:MeOH, 2:1 (15 mL). Separately, the free base C-isomer (21.8 mg, 0.0051 mmol) was added to a flask containing Zn(OAc)₂ (7.4 mg) in CHCl₃:MeOH, 2:1 (15 mL). Each solution was refluxed for 4 h (TLC control, SiO₂, 98:2 CH₂Cl₂:MeOH). The solvent was removed, and each mixture was taken up in CH₂Cl₂ and extracted with water and then brine. The organic layer was dried over Na₂SO₄. The solvent was removed to give the metal-containing **8-S** (19 mg, 91%), and C-isomer **8** (20 mg, 88%). **8-S**: mp > 275 °C; ¹H NMR (toluene-*d*₈, 330 K): δ 9.65 (br s, 4H), 9.02 (s, 4H), 8.32–8.0 (m, 9H), 7.75 (m, 30H), 6.30 (t, 2H, J = 7.6 Hz), 6.14 (t, 4H, J = 7.6 Hz), 5.32 (br s, 2H), 2.50–2.12 (m, 22H), 1.85–0.58 (m, 264H); UV/vis (toluene): λ 420, 480, 556, 606, 655; MALDI-TOF m/z 4378 ([M + H]⁺, calcd for C₂₇₂H₃₂₀N₂₀O₂₈ZnH 4379.4). **8**: mp > 275 °C; ¹H NMR (toluene-*d*₈, 330 K): δ 9.63 (br s, 4H), 9.02 (s, 4H), 8.35–8.0 (m, 9H), 7.75 (m, 30H), 6.29 (br t, 2H), 6.13 (br t, 4H), 5.19 (br s, 2H), 2.45–2.12 (m, 22H), 1.85–0.58 (m, 264H); UV/vis (toluene): λ 415, 470, 555, 605, 657; MALDI-TOF m/z 4378 ([M + H]⁺, calcd for C₂₇₂H₃₂₀N₂₀O₂₈ZnH 4379.4). Analogously, porphyrins **7** and **13** were obtained.

Porphyrin-monocavitand (7): metal-free porphyrin: yield 42%; ¹H NMR (benzene-*d*₆, 330 K): δ 9.82 (s, 2H), 9.28 (s, 2H), 8.96 (d, 2H, J = 4.8 Hz), 8.85–8.82 (m, 4H), 8.17 (s, 4H), 8.10 (d, 4H, J = 6.7 Hz), 8.03 (s, 2H), 7.85 (br s, 2H), 7.71–7.52 (m, 12H), 7.51–7.43 (m, 10H), 7.40 (s, 2H), 7.28 (s, 2H), 6.37 (t, 1H, J = 8.1 Hz), 6.23 (t, 2H, J = 8.1 Hz), 5.20 (t, 1H), 2.50–2.22 (m, 14H), 2.21–2.12 (m, 2H), 1.97–1.80 (m, 8H), 1.70–1.50 (m, 6H), 1.53 (s, 10H), 1.51–1.18 (m, 86H), 1.05–0.72 (m, 52H), 0.68–0.60 (m, 8H), –2.13 (s, 2H); MALDI-TOF m/z 2889 av ([M]⁺, calcd for C₁₈₈H₂₃₆N₁₂O₁₄ 2889). Zn-porphyrin **7**: Yield 91%; ¹H NMR (benzene-*d*₆, 330 K): δ 9.81 (s, 2H), 9.28 (s, 2H), 9.05 (d, 2H, J = 4.6 Hz), 8.98 (d, 2H, J = 4.6 Hz), 8.93 (s, 2H), 8.28–8.22 (m, 8H), 8.11 (s, 2H), 7.90–7.80 (br s, 2H), 7.79–7.42 (m, 26H), 6.36 (t, 1H, J = 8.1 Hz), 6.24 (t, 2H, J = 8.1 Hz), 5.08 (br t, 1H), 2.45–2.10 (m, 20H), 1.98–1.80 (m, 8H), 1.75–1.15 (m, 126H), 1.05–0.85 (m, 24H), 0.80–0.70 (m, 3H), 0.53–0.50 (m, 3H); FTIR (toluene, cm⁻¹): ν 3240, 1666, 1277, 1223, 1123, 1006, 797; UV/vis (toluene): λ 412, 450, 570, 612; MALDI-TOF m/z 2952 av ([M]⁺, calcd for C₁₈₈H₂₃₄N₁₂O₁₄Zn 2952).

Model porphyrin (13): metal-free porphyrin: yield 47%; ¹H NMR (CDCl₃, 295 K): δ 8.9 (dd, 4H, J = 4.4 Hz, $\Delta\nu$ = 10.6 Hz), 8.70 (s, 2H), 8.20 (d, 4H, J = 6.8 Hz), 8.15 (d, 4H, J = 7.2 Hz), 7.85 (t, 2H, J = 7.5 Hz), 7.80–7.75 (m, 10H), 7.06 (s, 2H), 4.10 (s, 6H), –2.61 (s,

2H); HRMALDI-FTMS m/z 777.2951 ([M + H]⁺, calcd for C₅₂H₃₆N₆O₂H 777.2973, error = 2.8 ppm). Zn-porphyrin **13**: yield 33%; ¹H NMR (toluene-*d*₈, 295 K): δ 9.00 (d, 2H, J = 4.6 Hz), 8.95 (d, 2H, J = 4.6 Hz), 8.91 (s, 2H), 8.33 (d, 4H, J = 7.1 Hz), 8.25–8.23 (m, 4H), 7.85 (t, 2H, J = 7.4 Hz), 7.79–7.75 (m, 4H), 7.55–7.52 (m, 6H), 7.27 (s, 2H), 3.51 (s, 6H); HRMALDI-FTMS m/z 839.2076 ([M + H]⁺, calcd for C₅₂H₃₄N₆O₂ZnH 839.2107, error = 3.7 ppm).

General Procedure for the Preparation of Ester and Amide Guests (14, 15, 16a, 17a,b–19). The acid chloride (1 equiv) (2 equiv for guest *ster*) was dissolved in EtOAc (2–3 mL) and added to a rapidly stirred mixture of the amine (1 equiv) and K₂CO₃ (2 equiv) in a 1:1 EtOAc/H₂O mixture (50 mL). The guest precipitated from the reaction mixture in each case. After 2 h, the mixture was filtered and the solid residue recrystallized from toluene to give **14**, **15**, **16a**, **17a,b**, **18**, and **19** as white solids in 27–90% yields.

2-(1-Adamantanyl)-N-benzyl-ethanamide (14): mp 167–168 °C; ¹H NMR (CDCl₃, 295 K): δ 7.29–7.26 (m, 2H), 7.23–7.19 (m, 3H), 5.57 (br s, 1H), 4.37 (d, 2H, J = 5.6 Hz), 1.90 (s, 5H), 1.66–1.62 (m, 3H), 1.57 (s, 9H); ¹³C NMR (CDCl₃, 295 K): δ 171.0, 138.6, 128.9, 128.1, 127.6, 52.0, 43.8, 42.8, 36.9, 33.0, 28.8; HRMALDI-FTMS m/z 284.2016 ([M]⁺, calcd for C₁₉H₂₅NOH 284.2009, error = 2.5 ppm).

N-(Pyridin-3-ylmethyl)-hexanamide (15): mp 56–57 °C; ¹H NMR (toluene-*d*₈, 295 K): δ 8.39–8.35 (m, 2H), 7.18–7.16 (m, 1H), 6.69–6.65 (m, 1H), 4.56 (br s, 1H), 3.93 (d, 2H, J = 6.1 Hz), 1.69 (t, 2H, J = 7.7 Hz), 1.51 (p, 2H, J = 7.4 Hz), 1.23–1.10 (m, 4H), 0.85 (t, 3H, J = 7.1 Hz); ¹³C NMR (CDCl₃, 295 K): δ 173.5, 149.1, 148.7, 135.7, 134.5, 123.7, 40.9, 36.6, 31.5, 25.5, 22.5, 14.0; HRMALDI-FTMS m/z 207.1492 ([M]⁺, calcd for C₁₂H₁₈N₂OH 207.1492, error = 0.0 ppm).

N-(1-Adamantyl)-nicotinamide (16a): mp 164–165 °C; ¹H NMR (toluene-*d*₈, 295 K): δ 8.92 (s, 1H), 8.50 (s, 1H), 7.87 (s, 1H), 6.72 (s, 1H), 5.25 (br s, 1H), 2.25–2.15 (m, 6H), 2.05–1.97 (m, 3H), 1.65–1.58 (m, 6H); ¹³C NMR (CDCl₃, 295 K): δ 164.8, 152.0, 147.8, 135.1, 131.7, 123.6, 52.9, 41.7, 36.4, 29.6; HRMALDI-FTMS m/z 257.1639 ([M + H]⁺, calcd for C₁₆H₂₀N₂OH 257.1648, error = 3.5 ppm).

Adamantanecarboxylic acid N-(pyridin-3-ylmethyl)-amide (17a): mp 120–122 °C; ¹H NMR (toluene-*d*₈, 295 K): δ 8.43 (s, 1H), 8.39 (d, 1H, J = 5.0 Hz), 7.21 (d, 1H, J = 7.6 Hz), 6.73–6.69 (m, 1H), 5.27 (br s, 1H), 4.05 (d, 2H, J = 5.8 Hz), 1.78 (s, 3H), 1.66–1.60 (m, 6H), 1.58–1.45 (m, 6H); ¹³C NMR (CDCl₃, 295 K): δ 178.3, 149.0, 148.8, 135.6, 134.6, 123.7, 40.9, 40.8, 39.4, 36.5, 28.2; HRMALDI-FTMS m/z 271.1806 ([M]⁺, calcd for C₁₇H₂₂N₂OH 271.1805, error = 0.4 ppm).

2-(1-Adamantyl)-N-pyridin-3-ylmethyl-ethanamide (17b): mp 131–132 °C; ¹H NMR (toluene-*d*₈, 295 K): δ 8.41 (s, 1H), 8.38 (d, 1H, J = 4.0 Hz), 7.22 (d, 1H, J = 7.8 Hz), 6.70–6.67 (m, 1H), 4.72 (br s, 1H), 3.96 (d, 2H, J = 6.1 Hz), 1.88–1.85 (br s, 3H), 1.64–1.53 (m, 14H); ¹³C NMR (CDCl₃, 295 K): δ 171.2, 149.3, 149.0, 135.9, 134.4, 123.7, 51.8, 42.8, 41.1, 36.8, 33.0, 28.7; HRMALDI-FTMS m/z 285.1953 ([M]⁺, calcd for C₁₈H₂₄N₂OH 285.1961, error = 2.8 ppm).

3,5-Pyridine diester (18): mp 90–92 °C; ¹H NMR (toluene-*d*₈, 295 K): δ 8.49 (s, 2H), 7.32 (s, 1H), 4.74 (s, 4H), 1.91 (s, 4H), 1.83 (s, 6H), 1.60–1.56 (m, 6H), 1.53–1.51 (m, 18H); ¹H NMR (CDCl₃, 295 K): δ 8.56 (s, 2H), 7.67 (s, 1H), 5.10 (s, 4H), 2.10 (s, 4H), 1.93 (br s, 6H), 1.68–1.64 (m, 6H), 1.60–1.55 (m, 18H); ¹³C NMR (CDCl₃, 295 K): δ 171.6, 149.4, 136.0, 131.9, 63.1, 48.8, 42.5, 36.9, 33.1, 28.7; HRMALDI-FTMS m/z 492.3106 ([M + H]⁺, calcd for C₃₁H₄₁N₃O₄H 492.3108, error = 0.4 ppm).

3,5-Pyridine diamide (19): mp 193–194 °C; ¹H NMR (CDCl₃, 295 K): δ 8.42 (br s, 2H), 7.56 (s, 1H), 5.85 (br t, 2H), 4.41 (d, 4H, J = 6 Hz), 1.96 (s, 4H), 1.93 (br s, 6H), 1.68–1.64 (m, 6H), 1.60–1.55 (m, 18H); ¹³C NMR (CDCl₃, 313 K): δ 171.4, 148.6, 135.4, 52.0, 43.1, 41.2, 37.1, 33.3, 29.0; HRMALDI-FTMS m/z 490.3415 ([M + H]⁺, calcd for C₃₁H₄₃N₃O₂H 490.3428, error = 2.7 ppm).

General Procedure for the preparation of Amide Guests (16b–e). The corresponding acid (1 equiv), the amine (1 equiv), DCC (1 equiv), and a catalytic amount of DMAP (~5 mg) were suspended in anhydrous THF (75 mL). The mixture was stirred for 2 days at 35 °C. The solvent was removed in vacuo, and the solid residue was dissolved in EtOAc and washed with water and brine. The organic layer was dried over MgSO₄, the solvent was then removed in vacuo, and the

product was purified by column chromatography (EtOAc) to give the amides **16b–e** as white solids in 40–70% yields.

N-(1-Adamantyl)-2-(pyridin-3-yl)ethanamide (16b): mp 174–175 °C; ¹H NMR (toluene-*d*₈, 295 K): δ 8.39 (s, 2H), 7.27 (d, 1H, *J* = 7.6 Hz), 6.72–6.68 (m, 1H), 2.85 (s, 2H), 1.82–1.77 (m, 9H), 1.49–1.43 (m, 6H); ¹³C NMR (CDCl₃, 295 K): δ 168.9, 150.2, 148.4, 136.8, 131.4, 123.6, 52.3, 41.6, 41.6, 36.3, 29.4; HRMALDI-FTMS *m/z* 271.1798 ([M]⁺, calcd for C₁₇H₂₂N₂OH 271.1805, error = 2.6 ppm).

N-(1-Adamantyl)-3-(pyridin-3-yl)propanamide (16c): mp 148–149 °C; ¹H NMR (toluene-*d*₈, 295 K): δ 8.41–8.36 (m, 2H), 7.09 (s, 1H), 6.72–6.69 (m, 1H), 2.65 (t, 2H, *J* = 7.4 Hz), 1.87 (s, 9H), 1.79 (t, 2H, *J* = 7.3 Hz), 1.55–1.48 (m, 6H); ¹³C NMR (CDCl₃, 295 K): δ 170.5, 149.9, 147.7, 136.6, 136.3, 123.5, 52.1, 41.7, 38.9, 36.4, 29.5, 28.9; HRMALDI-FTMS *m/z* 285.1954 ([M + H]⁺, calcd for C₁₈H₂₄N₂OH 285.1961, error = 2.5 ppm).

N-(1-Adamantylmethyl)-2-(pyridin-3-yl)ethanamide (16d): mp 108–110 °C; ¹H NMR (toluene-*d*₈, 295 K): δ 8.47 (s, 1H), 8.35 (d, 1H, *J* = 4.7 Hz), 7.38 (d, 1H, *J* = 7.7 Hz), 6.76–6.70 (m, 1H), 5.65 (br s, 1H), 3.10 (s, 2H), 2.84 (d, 2H, *J* = 6.5 Hz), 1.81 (s, 3H), 1.54 (dd, 6H, *J* = 12.1 Hz, Δ*ν* = 46.1 Hz), 1.28 (s, 6H); ¹³C NMR (CDCl₃, 295 K): δ 170.0, 150.4, 148.8, 137.0, 131.2, 123.8, 51.3, 41.0, 40.3, 37.0, 33.9, 28.2; HRMALDI-FTMS *m/z* 285.1953 ([M + H]⁺, calcd for C₁₈H₂₄N₂OH 285.1961, error = 2.8 ppm).

N-(1-Adamantylmethyl)-3-(pyridin-3-yl)propanamide (16e): mp 92–93 °C; ¹H NMR (toluene-*d*₈, 295 K): δ 8.41–8.35 (m, 2H), 7.10

(s, 1H), 6.72–6.69 (m, 1H), 2.80 (t, 2H, *J* = 6.5 Hz), 2.70 (t, 2H, *J* = 7.4 Hz), 1.94 (t, 2H, *J* = 7.3 Hz), 1.82 (s, 3H), 1.55 (dd, 6H, *J* = 12.1 Hz, Δ*ν* = 50.6 Hz), 1.22 (s, 6H); ¹³C NMR (CDCl₃, 295 K): δ 171.5, 149.9, 147.8, 136.5, 136.3, 123.5, 51.1, 40.5, 38.2, 37.0, 33.7, 29.0, 28.3; HRMALDI-FTMS *m/z* 299.2129 ([M + H]⁺, calcd for C₁₉H₂₆N₂OH 299.2118, error = 3.7 ppm).

Determination of the Association Constant. Binding studies were performed in toluene solution at 295 ± 1 K. An aliquot from the stock solution of compounds **15–19** was added to the sample cell (1 mL) containing hosts **7**, **8**, or **13** and after homogenization, the absorption spectrum was recorded. Additional aliquots of **15–19** were added, and the spectrum was recorded after each addition. Host concentration [7] = [8] = [13] = 4.5 × 10⁻⁶ M, guest concentration range 2.0 × 10⁻⁶ – 8.0 × 10⁻⁵ M. The association constant was calculated from the absorption intensity changes by nonlinear regression analysis. Error 10%. All experiments were performed at least in duplicate.

Acknowledgment. We are grateful for financial support from the Skaggs Research Foundation and the National Institutes of Health. We thank Professor Dr. F. N. Diederich of ETH, Zürich for providing us with the curve-fitting program. Dr. A. Rafai Far is acknowledged for experimental advice.

JA010038R